Development 127, 605-619 (2000)
Printed in Great Britain © The Company of Biologists Limited 2000
DEV4275

Combinatorial signaling through BMP receptor IB and GDF5: shaping of the distal mouse limb and the genetics of distal limb diversity

Scott T. Baur, Jia J. Mai and Susan M. Dymecki*

Department of Genetics, Harvard Medical School, Boston, MA 02115, USA
*Author for correspondence (e-mail: dymecki@rascal.med.harvard.edu)

Accepted 5 November 1999; published on WWW 12 January 2000

SUMMARY

In this study, we use a mouse insertional mutant to delineate gene activities that shape the distal limb skeleton. A recessive mutation that results in brachydactyly was found in a lineage of transgenic mice. Sequences flanking the transgene insertion site were cloned, mapped to chromosome 3, and used to identify the brachydactyly gene as the type *IB bone morphogenetic protein receptor, BmprIB (ALK6)*. Expression analyses in wild-type mice revealed two major classes of *BmprIB* transcripts. Rather than representing unique coding RNAs generated by alternative splicing of a single pro-mRNA transcribed from one promoter, the distinct isoforms reflect evolution of two *BmprIB* promoters: one located distally, driving expression in the developing limb skeleton, and one situated proximally, initiating transcription in neural epithelium. The distal promoter is deleted in the insertional mutant, resulting in a regulatory allele (*BmprIB^{Tg}*) lacking *cis*-sequences necessary for limb *BmprIB* expression. Mutants fail to generate digit cartilage, indicating that BMPRIB is the physiologic transducer for the formation of digit cartilage from the skeletal blastema. Expansion of *BmprIB* expression into the limb through acquisition of these distal *cis*-regulatory sequences appears, therefore, to be an important genetic component driving morphological diversity in distal extremities. GDF5 is a BMP-related signal, which is also required for proper digit formation. Analyses incorporating both *Gdf5* and *BmprIB^{Tg}* alleles revealed that BMPRIB regulates chondrogenesis and segmentation through both GDF5-dependent and -independent processes, and that, reciprocally, GDF5 acts through both IB and other type I receptors. Together, these findings provide in vivo support for the concept of combinatorial BMP signaling, in which distinct outcomes result both from a single receptor being triggered by different ligands and from a single ligand binding to different receptors.

Key words: Signaling, BMP receptor, GDF5, Apoptosis, Skeletal morphogenesis, Digit formation, Mouse

INTRODUCTION

The cartilage template through which the limb skeleton forms, results from the iteration of three basic processes: condensation of chondrogenic cells to form a focus, bifurcation of the focus to generate Y-shaped elements and axial segmentation to produce subelements. This program begins with a single de novo mesenchymal condensation – the anlagen of the humerus (or femur in the hindlimb) – and proceeds in a proximodistal direction. First, the condensation grows distally by appropriating nearby mesenchymal cells into the focus. The distal end then branches and segments to form the ulna and radius (tibia and fibula); these, in turn, elongate, branch and segment to form the proximal carpals (tarsals). The axis of development now switches from proximodistal to posteroanterior with the ulna giving rise to the perpendicularly oriented axis of the digital arch, comprising distal carpals and metacarpals (distal tarsals and metatarsals). Each metacarpal (metatarsal), also referred to as a digital ray, then segments axially to form the phalanges. Most elements of the limb are, therefore, thought to arise by ordered branching and segmentation of preexisting chondrogenic elements (Oster et al., 1988; Shubin and Alberch, 1986).

The de novo condensation within the early limb bud results from interactions between mesenchyme and ectoderm and involves a number of secreted molecules, including FGFs (Martin, 1998), Wnts (Kengaku et al., 1998; Parr et al., 1993; Tickle, 1995) and BMPs (Hogan, 1996; Kingsley, 1994). Surrounding mesenchyme is then recruited into the chondrogenic condensation in what appears to be an autocatalytic process – as the density of chondrogenic cells increases, further aggregation is enhanced, which in turn increases recruitment of chondrogenic cells (Shubin and Alberch, 1986). Aggregation favors the distal end of the element where the adjacent progress zone provides proliferating mesenchyme. In contrast, proximal and lateral recruitment is restricted by a more limited supply of mesenchyme, and by differentiation of the outerzone of the condensation into a tangentially stacked cell layer, the perichondrium, which separates the cartilage element from its

mesenchyme surround (Caplan and Pechack, 1987). As the condensation elongates, it eventually reaches a size and stage where the more proximal region differentiates, while the distal domain continues to recruit chondrogenic cells. By this stage, the cartilage element is polarized, with the immature distal end acting as a stronger focus for condensation than the more differentiated proximal end. Together with tightly controlled cell death, the outcome is segmentation of the element between the more and less differentiated domains into two subelements; these subelements will go on to differentiate and articulate with each other in a synovial joint. Cartilage condensation and segmentation are, therefore, highly coordinated processes organized in both space and time.

Secreted signaling molecules of the TGFβ family, such as bone morphogenetic proteins (BMPs) and growth/differentiation factors (GDFs), can affect the outcome of these linked processes of chondrogenesis and cleavage; the result being alterations in both bone shape and number (Hogan, 1996; Kingsley, 1994). BMPs were first discovered as proteins that induce ectopic endochondral bone formation (Hogan, 1996 and references therein). Compatible with such activity, BMP2-BMP7 were found to be expressed in discrete regions of the developing skeleton. GDF5-GDF7 were identified by their homology to BMPs and also show characteristic patterns of expression in the developing skeleton (Storm et al., 1994). BMPs and GDFs appear to bind similar receptors. These include various type I and type II transmembrane serine-threonine kinases (Yamashita et al., 1996). Type I receptors (TSR1=ALK1; ACTRI=ALK2; BMPrIA = ALK3, BRKI; BMPrIB = ALK6, BRKII and RPKI) transmit the BMP or GDF signal to intracellular phosphorylation cascades involving members of the Smad family (Hoodless et al., 1996; Liu et al., 1996; Massague, 1996). Type II receptors (BMPrII = BRK3) act to facilitate both ligand binding and signal transmission through type I receptors. Recent data indicates that ligand binding can induce the formation of heterotetrameric complexes consisting of two type I receptors and two type II receptors (Yamashita et al., 1994). Thus, the repertoire of potential ligand-receptor interactions is considerable.

BMPrIA and BMPrIB are of particular interest for understanding the regulation of skeletogenesis. *BmprIA* mRNA can be detected in the limb progress zone, interdigital mesenchyme, periarticular perichondrium and differentiated hypertrophic chondrocytes (Zou et al., 1997). From misexpression studies, two different functions have been proposed for BMPrIA: regulation of chondrocyte differentiation (Zou et al., 1997) and signaling interdigital cell death (Yokouchi et al., 1996). In contrast to IA, *BmprIB* is expressed in the earliest chondrogenic condensations (Kawakami et al., 1996; Zou et al., 1997) and has been hypothesized to control mesenchyme aggregation and cartilage formation (Enomoto-Iwamoto et al., 1998; Kawakami et al., 1996; Merino et al., 1998; Zou et al., 1997). Although not normally expressed in interdigital mesenchyme, misexpression of a constitutively active IB receptor (caBMPRIB) in this region has also been shown capable of inducing cell death (Zou et al., 1996, 1997). While the misexpression experiments have been informative in defining a range of activities these receptors possess, the physiological functions for the IA and IB receptors remain to be defined.

Here we report a mouse insertional mutant in which cartilage condensation and segmentation of the distal limb are disrupted, thereby providing a unique opportunity to define gene activities critical to these processes. Through positional cloning, we show that this insertion mutation is a regulatory allele of the *BMP receptor IB* gene (*BmprIB*^{Tg}) and that this allele is null with respect to the limb. Our results show that BMPrIB is the physiological transducer mediating the development of digit cartilages and that this differentiation program is initiated through the binding of GDF5. While digit chondrogenesis appears to require this particular receptor-ligand pair, we show

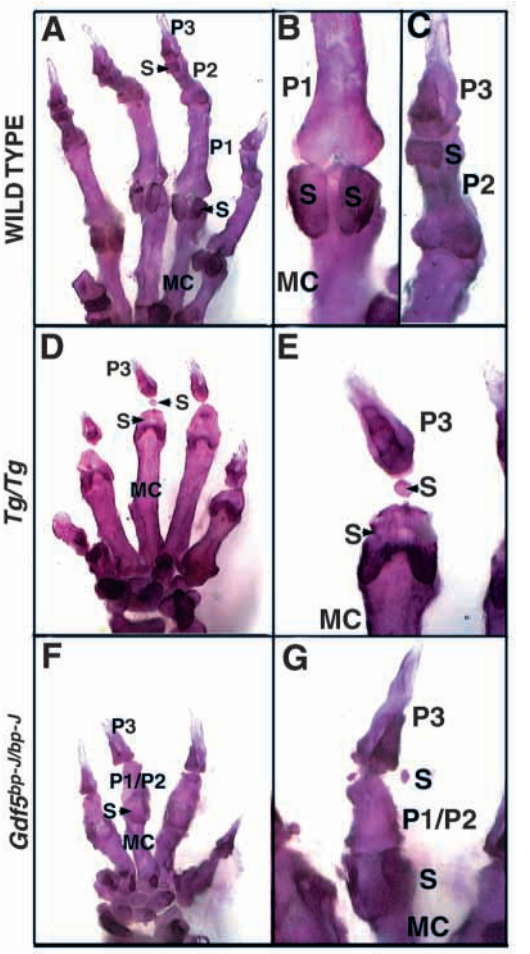

Fig. 1. Transgene insertion uncovers brachydactyly locus. Adult forelimbs stained with Alizarin red. (A-C) Wild-type (WT) forefoot; (D,E) insertional mutant (*Tg/Tg*); (F,G) *brachypod* (*Gdf5*$^{bp\text{-}J/bp\text{-}J}$). (A-E) Ventral forefoot. Insertional mutant comprises normal metacarpals but is missing the basal (P1) and medial (P2) phalanges. In the WT forefoot (A), sesamoid (S) bones can be seen at the metacarpophalangeal joints and the distal phalangeal joints (P2-P3). (B,C) Higher magnification of the joint regions shown in A. (D) In the insertional mutant, note the fused V-shaped metacarpophalangeal sesamoid, the absence of P1 and P2 phalanges, and the reduction in size of the distal sesamoid. (E) Higher magnification of an MC-P3 joint from D. (F) Ventral forefoot from *Gdf5*$^{bp\text{-}J/bp\text{-}J}$ mice. As reported elsewhere (Gruneberg and Lee, 1973; Storm et al., 1994), metacarpals are significantly reduced in length, rudimentary phalanges (P1/P2) replace P1 and P2. (G) Higher magnification of a distal digit showing fused metacarpophalangeal sesamoids and a rudimentary P1/P2 element.

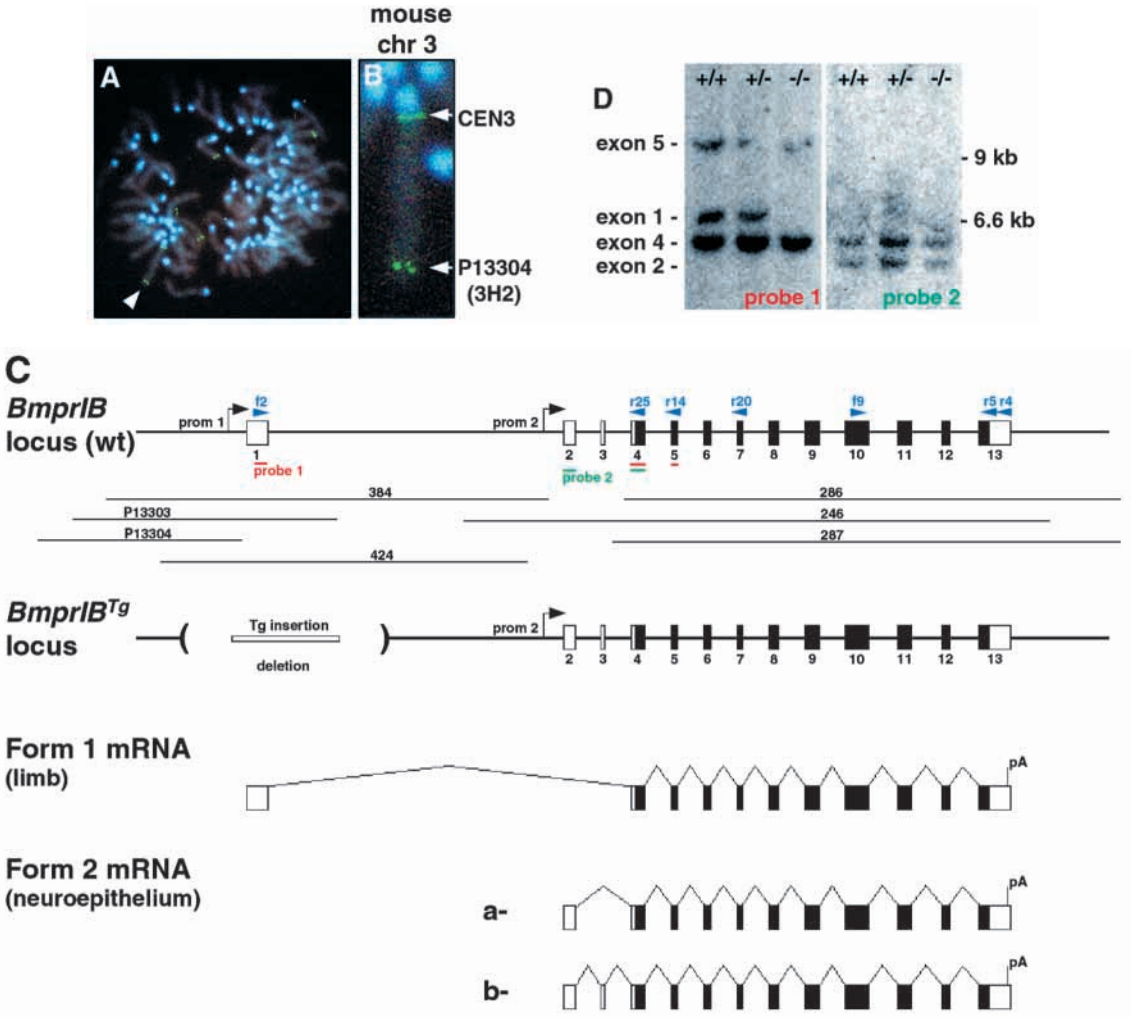

Fig. 2. Transgene insertion on mouse chromosome 3 disrupts the *BmprIB* gene. (A,B) Double labeling of wild-type metaphase chromosome spreads with insertion probe P13304 and a centromere 3-specific probe. (B) Higher magnification of the chromosome in A marked by an arrowhead. The insertion is located at a position that is 91% of the distance from the centromere to the telomere of chromosome 3, corresponding to band H2. By nucleotide sequence, insertion probe P13304 was syntenic to human chromosome 4q21. (C) Structure of the wild-type (wt) *BmprIB* gene and the transgenic allele $BmprIB^{Tg}$. In $BmprIB^{Tg}$, a random transgene insertion was accompanied by a deletion including exon 1. Upper, arrangement of *BmprIB* exons. Exons are depicted by black boxes, untranslated sequence by white boxes. The location of fragments used as probes in Southern blotting are shown below, and primers used in RT-PCR and 5′ RACE are marked above. Exons were identified using published *BmprIB* cDNA sequence as reference, along with the novel cDNAs identified by 5′ RACE (diagrammed at figure bottom). The cDNA sequence has been renumbered to account for the newly identified 5′ exons (1-3). Sequences corresponding to exon 1 are 1-283; exon 2, 284-437; exon 3, 438-521; exon 4, 522-681; exon 5, 682-786; exon 6, 787-887; exon 7, 888-985; exon 8, 986-1123; exon 9, 1124-1315; exon 10, 1317-1612; exon 11,1613-1790; exon 12,1797-1921; exon 13,1922-2345. Exon 1 is situated more than 20-kb upstream of exon 2. The extracellular domain is encoded in exons 4-6, the transmembrane domain in exon 7, the GS box in exon 8, and the kinase domain in exons 9-13. The entire *BmprIB* gene is contained within a BAC contig of ~200-kb (depicted as overlapping black lines below the wt locus). 5′ RACE identified two classes of *BmprIB* transcripts: exon 1-containing mRNAs are designated form 1 and represent the only mRNAs isolated from embryonic limb; exon 2-containing mRNAs, designated form 2 (a and b), predominate in neuroepithelium. These two RNA classes are transcribed from two distinct promoters; a distal promoter immediately upstream from exon 1 (prom 1), and a proximal promoter, adjacent to exon 2 (prom 2). Lines indicate the splicing patterns for the three transcripts. (D) Southern blot analysis of genomic DNA showing loss of *BmprIB* exon 1. DNA isolated from a wt (+/+) animal, $BmprIB^{Tg}$ homozygote (–/–), and $BmprIB^{Tg}$ heterozygote (+/–).

that BMPRIB and GDF5 each regulate additional aspects of skeletal morphogenesis through other partners.

To evaluate the molecular nature of the $BmprIB^{Tg}$ allele, we have determined the structure of the mouse *BmprIB* gene and have discovered that its transcription initiates from two distinct promoters: one that drives expression in neuroepithelium and one, located more than 20 kb upstream, which is required for expression in the developing limb skeleton. The generation of this distal regulatory element may have been a critical event in the genetic evolution of distal limb form.

MATERIALS AND METHODS

Identification of the insertion locus

To clone DNA flanking the transgene insertion, we synthesized

genomic libraries (λFixII and λZap vectors, Stratagene) using kidney DNA isolated from transgenic animals. Primers derived from 3′ flanking DNA sequence were used to screen P1 and BAC mouse genomic libraries by PCR (Genome Systems). Primer sequences: SD140, CTCAGCATTAGCATTTCC; SD142, GCTGTTGGTATGGGACGG. P1 clone 13304 was used as a fluorescence in situ hybridization probe to localize the transgene insertion to mouse chromosome 3 (Genome Systems).

Structure of the *BmprIB* gene

The murine *BmprIB* cDNA (GenBank Z23143) was cloned from a 13.5 days post coitum (dpc) embryonic cDNA library (GIBCO BRL) by RT-PCR and used to screen BAC mouse genomic libraries by hybridization (Research Genetics). Positions of exons were determined directly, by nucleotide sequence (Biopolymers Facility, Howard Hughes Medical Institute, Harvard Medical School), or indirectly, by Southern blot analysis of BAC and genomic DNA. *BmprIB* region-specific radiolabeled probes were generated from cloned (TA Cloning Kit, Invitrogen) RT-PCR products. Primer sequences (F indicates forward; R, reverse) for probe 1 (Fig. 2C): F2, CATTTGGCGCTGAGCTATGAC; R14, GACATCCAGAGGTGACAACAG; for probe 2: F-AUAP (GIBCO BRL, RACE anchor primer), GGCCACGCGTCGACTAGTAC; R25, ATATTGTTGACTGAGTCTTCC. End-specific probes were used to orient the BAC and P1 genomic clones and grossly delineate the deletion caused by the transgene insertion. Assembly of DNA sequences, conceptual translation and sequence alignments were performed using LaserGene Navigator (DNASTAR). Sequence comparisons with the GenBank database were performed using the BLAST network services.

Mice and genotyping

Genotyping for the 4917^{Tg} ($BmprIB^{Tg}$) allele was performed by Southern blot analysis of *Hin*dIII-digested yolk sac or tail DNA (Dymecki, 1996) probed with radiolabeled junctional fragments from insertion clone P13303. The $Gdf5^{bp\text{-}J}$ allele occurred spontaneously in the A/J strain (Jackson Laboratory) and contains an insertion of a guanine residue. $Gdf5^{bp\text{-}J}$ allele detection was by PCR analysis of tail DNA. Primer sequences: wild-type FSB50, GCGGAAACGCCGGGC-3′; *bp-J*, FSB51, GCGGAAACGCCGGGG; RSB52, GTGGGAGCGCAAGGGG.

Transcript detection

Total RNA (RNeasy, Qiagen) isolated from embryonic tissues at 13.5 dpc, was used for RACE PCR (GIBCO-BRL) to obtain 5′ ends of *BmprIB* cDNAs. *BmprIB*-reverse primers for cDNA syntheses: R20, AGACAGTCACAGAGATAAGC (RACE); R4, CCATGATGAATCCGTGTTTC (RT-PCR). *BmprIB*-reverse primers for nested RACE PCR were R14 and R25. Detection of *BmprIB* cDNAs by RT-PCR was performed using the region-specific primers: F9, GGCAAGCCAGCAATCGCCCATC; R5, TCTTCCAGGAAAGTCTGAACT; F2; R14. In situ hybridization on cryosections (20 μm) of embryonic tissue at 12.5-13.5 dpc with sense or antisense digoxigenin (Boehringer Mannheim)-labeled riboprobes was performed as described (Bau and Cepko, 1997). Riboprobes were as described previously: *BmprIB* (Zou et al., 1997), *BmprIA* (Zou et al., 1997), *ColaI(II)* (Lee et al., 1996), *Gdf5* (Storm et al., 1994), *Gli1* (Hui et al., 1994), *Gli2* (Hui et al., 1994), *Gli3* (Hui et al., 1994), *Ihh* (Bitgood and McMahon, 1995).

Skeletal preparations and histology

Skeletons of adult mice were prepared in 2% (w/v) potassium hydroxide and stained with Alizarin red (Green, 1968). To quantitate bone length, metatarsals were imaged, measured and compared between gender-matched mutant and wild-type siblings using a paired Student's *t*-test. For Alcian blue histology, mouse limbs (12.5-16.5 dpc) were fixed in 4% paraformaldehyde/PBS overnight at 4°C, dehydrated and embedded in paraffin. 6 μm sections were mounted on glass slides, deparaffinized, rehydrated and stained for 3 hours (1% Alcian blue, 3% acetic acid).

Proliferation and apoptosis assays

Pregnant mice were injected intraperitoneally with 50 μg BrdU/gm body weight 1.5 hours before killing. Limbs (11.5-14.5 dpc) were processed as previously described for paraffin. Immunocytochemical detection of BrdU (Amersham Pharmacia Biotech) was performed on 6 μm sections as described (Nowakowski et al., 1989) with the addition of a Trypsin/EDTA permeabilization step (St-Jacques et al., 1999). Positive cells were visualized through peroxidase staining using diaminobenzidine (DAB) and then counterstained with hematoxylin. To quantitate the rate of cell proliferation, serial images of the same digit were collected and BrdU-positive (black) and -negative (gray) cells in the phalangeal region (Fig. 7E,F) were counted in two wild-type and two *Tg/Tg* littermate embryos at 13.5 dpc. The significance of the percentages was determined using the Student's *t*-test. Apoptosis was detected by terminal deoxynucleotidyl transferase-mediated dUTP nick-end labeling (Boehringer Mannheim). Fluorescent images of fluorescein-dUTP incorporation were captured prior to immunocytochemical detection. Peroxidase staining with DAB was then performed to facilitate quantitation of labeled cells as for the BrdU assay.

RESULTS

Brachydactyly in 4917^{Tg} homozygotes

The 4917^{Tg} mouse line was produced by microinjection of transgene DNA into fertilized eggs (Dymecki, 1996). Southern blot analyses showed that heterozygotes harbored two copies of the 7 kb transgene in a head-to-tail configuration (data not shown). Heterozygotes were normal and fertile, and transmitted the transgene in a Mendelian fashion. Homozygosity for the transgene insertion caused neither embryonic nor postnatal lethality, as the predicted Mendelian ratio of alleles was observed among adult mice. Pups appeared and behaved outwardly normal, with the exception that homozygotes displayed brachydactyly (short digits).

Skeleton preparations revealed that 4917^{Tg} homozygotes show two highly penetrant phenotypes: complete loss of proximal (P1) and medial (P2) phalanges in all digits (I-V) of both the forelimb and hindlimb, and fusion of the small sesamoid bones that normally articulate with these missing elements (Fig. 1). Although not fully penetrant, on average $4917^{Tg/Tg}$ metatarsals were approximately 90% (±5% s.d.) the length of wild-type ($P<0.005$, Student's *t*-test, $n=42$). Most other bones in the forefoot and hindfoot appeared normal in size, shape and number, including the terminal phalanges (P3). The axial skeleton was unaffected. In the normal course of development, P1 and P2 phalanges arise by sequentially segmenting off the cartilaginous digital ray; in contrast, the P3 phalanges form directly from distal membrane rather than segmenting from more proximal elements (Gruneberg and Lee, 1993). 4917^{Tg} homozygotes show a specific loss of all endochondral-derived phalanges.

Sesamoids arise as secondary cartilages induced during embryonic movement, usually initiated and remodelled by changes in tension at a joint (Hinchliffe, 1994). In wild-type forefoot and hindfoot digits, sesamoid bones are found at the metacarpophalangeal (metatarsophalangeal) joints and at the distal phalangeal joints (P2-P3) (Fig. 1B,C). In 4917^{Tg}

homozygous forelimbs, each pair of metacarpophalangeal sesamoids were found to be fused at the distal ends, resulting in a forked configuration (Fig. 1E); the P2-P3 sesamoids were absent or reduced in overall size. In both the mutant forefoot and hindfoot, the absence of P1 and P2 phalanges generates a novel joint between P3, the fused sesamoids, and the metacarpal or metatarsal. Mechanical instability and tension associated with this unusual articulation likely induces these atypical sesamoid morphologies.

Null mutations in the *Gdf5* gene (*Gdf5*$^{bp\text{-}J}$) also result in brachydactyly. Although described in detail elsewhere (Gruneberg and Lee, 1973; Storm et al., 1994; Storm and Kingsley, 1996), *Gdf5*$^{bp\text{-}J}$ mutant limbs are presented for comparison (Fig. 1F,G). As reported, examination of the phalanges showed that P1 and P2 are replaced by a single rudimentary element (P1/P2) in *Gdf5*$^{bp\text{-}J}$ mutants. Rather than arising from the digital ray, these rudimentary elements are thought to derive from a cartilage template formed out of perichondrial-like dense mesenchyme located in the presumptive phalangeal region (Storm and Kingsley, 1999). This is in distinction to *4917*^{Tg} homozygotes where we observed a complete loss of P1 and P2 elements. Both mutants display unusual sesamoid morphologies. In addition to the phalangeal defect resulting in brachydactyly, the most striking anomaly in *Gdf5*$^{bp\text{-}J}$ mutants is a severe reduction in the length of many of the long bones of both the forelimb and hindlimb (Gruneberg and Lee, 1973; Storm and Kingsley, 1996). *Gdf5*$^{bp\text{-}J}$ mutant metarsals were approximately 44% (±5% s.d.) the length of wild-type (P<0.005, Student's t-test, n=12). Because these defects encompass more than just the digits, the *Gdf5* genomic site has been designated the *brachypodism (bp)* locus. Despite the differences between *4917*^{Tg} and *Gdf5*$^{bp\text{-}J}$ mutant limbs, the shared loss of digital ray-derived phalanges suggested that the *4917*^{Tg} and *Gdf5* loci may participate in common or parallel genetic pathways in vivo to pattern the distal limb.

4917^{Tg} insertion disrupts *BmprIB*

To clone the mutant and corresponding wild-type loci and identify the brachydactyly gene, a genomic library was prepared from *4917*^{Tg} mouse DNA and screened with a radiolabeled probe for the transgene. Clones containing both murine and transgene DNA were identified. Using the murine-specific DNA segments of these clones as probes, we isolated a series of overlapping wild-type genomic clones (recombinant P1 and BAC) which were polymorphic between wild-type and *4917*^{Tg} DNA, indicating that they mapped to the preinsertion locus (Fig. 2).

To identify candidate brachydactyly genes, the *4917*^{Tg} insertion was localized by fluorescence in situ hybridization of clone P13304 to the distal end of mouse chromosome 3, band H2 (Fig. 2A,B). Physical and genetic maps of mouse chromosome 3 show scattered synteny between mouse 3H2 and human chromosome region 4q21-25 (Mouse Genome Database, Jackson Laboratory). DNA sequence derived from insertion clone P13304 queried against a non-redundant sequence database (GenBank+EMBL+DDBJ+PDB sequences) showed significant homology (E=5e-20) to BAC clone B299F15 from human chromosome 4q21 (the Stanford Human Genome Center), consistent with the predicted synteny. The human *BMPRIB* gene was recently mapped to 4q23-24 (Astrom et al., 1999; Ide et al., 1998), making it a candidate brachydactyly gene.

Based on this synteny relationship and previous reports showing that *BmprIB* is expressed in developing digits (Dewulf et al., 1995), we cloned the mouse *BmprIB* cDNA from a 13.5 dpc embryonic library and used it to analyze gene structure in *4917*^{Tg} homozygotes. Through Southern analyses (Fig. 2D), we found that part of the 5′ untranslated region of the *BmprIB* gene is deleted in homozygous mutants and localizes to the preinsertion contig (Fig. 2C). Coding exons within the gene appeared intact. Wild-type DNA isolated from C57BL/6J, SJL and 129Sv showed no exon 1-specific polymorphisms, thereby excluding strain differences as causing the observed polymorphism (data not shown). Other than this deletion of less than 100 kb, the *4917*^{Tg} and wild-type genomes flanking the insertion site were found to be colinear as assessed by restriction mapping of the clones and genomic Southern analyses (data not shown).

Genomic organization of *BmprIB*

As a basis from which to evaluate the molecular nature of the *4917*^{Tg} insertion mutation, the structure of the wild-type murine *BmprIB* gene was determined. Molecular clones of the *BmprIB* gene were obtained from a mouse genomic BAC library by hybridizing to a radiolabeled *BmprIB* cDNA probe. Except for a portion of the 5′-untranslated region (nucleotides 1- 283) which was found on the preinsertion clones 384, 424 and P13303, the entire *BmprIB* cDNA was represented on the overlapping BAC 246 (Fig. 2C).

Gene structure is diagrammed in Fig. 2 (and will be reported in detail elsewhere). Using the published *BmprIB* cDNA sequence (GenBank Z23143) as reference along with the novel cDNAs identified by 5′ RACE reported below, we identified thirteen exons spanning ~200 kb. In the *4917*^{Tg} allele, exon 1 and flanking sequence from the *BmprIB* gene are deleted and together replaced with 14 kb of transgene DNA; we therefore refer to this allele as *BmprIB*^{Tg}. It is unlikely that genes other than *BmprIB* have been affected by the transgene insertion, as a targeted deletion of *BmprIB* exon 4 shows a very similar phenotype (Yi et al., 2000).

Distinct promoters drive *BmprIB* expression in limb cartilage versus neuroepithelium

Because of discrepancies between published *BmprIB* cDNA sequence and the genomic sequence obtained from BAC insertion clones 384 and 246, we used RACE to examine the 5′ ends of *BmprIB* transcripts found in different tissues. *BmprIB* is expressed in a variety of embryonic tissues at midgestation (Dewulf et al., 1995), most prominent being the chondrogenic condensations in the limb and vertebral bodies, and the neural tube and olfactory neuroepithelium. From these tissues, we isolated two major classes of *BmprIB* RNA (Fig. 2C). Those containing exon 1 were termed form 1 and were the only RNAs found in limb; those lacking exon 1, but containing exon 2, were called form 2 and were the predominant species identified in olfactory epithelium. Subcategories of form 2 RNAs have also been identified, differing by the absence (form 2a) or presence (form 2b) of exon 3. All three RNA species appear to differ only in the 5′-untranslated region. Rather than representing unique coding transcripts generated by alternative splicing of a single pro-

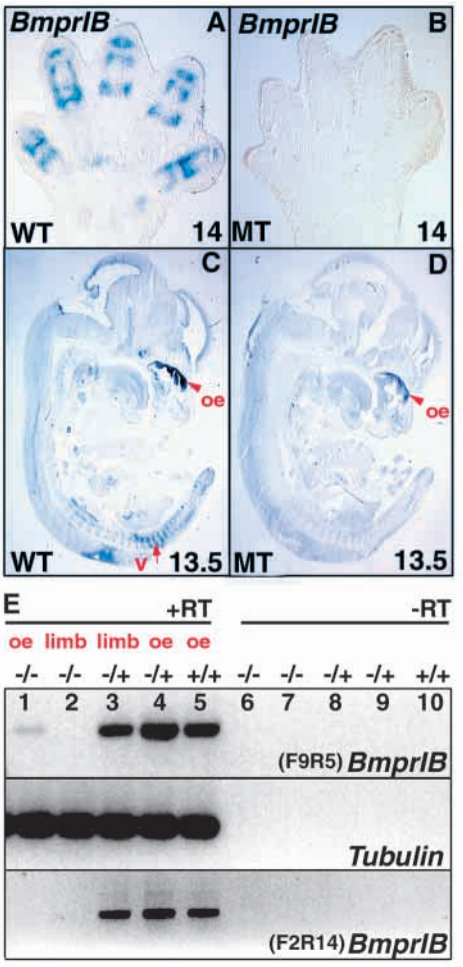

Fig. 3. Deletion of *cis*-sequences results in loss of *BmprIB* expression in the limb. (A-D) Digoxigenin in situ hybridization on sagittal sections through wild-type (A,C) and *BmprIB*$^{Tg/Tg}$ mutant (B,D) embryos. (A) Wild-type (WT) forelimb autopod at 14 days post coitum (dpc). At this stage *BmprIB* is strongly expressed in the outerzone of the phalangeal cartilage elements. (B) *BmprIB*$^{Tg/Tg}$ mutant (MT) forelimb autopod at 14 dpc. *BmprIB* transcripts are undetectable. (C) WT embryo at 13.5 dpc. Location of *BmprIB* expression includes the olfactory epithelium (oe; arrowhead), the neural tube, and the vertebral condensations (v, arrow). (D) MT embryo at 13.5 dpc. *BmprIB* expression remains detectable in the olfactory epithelium, but is lost from vertebrae. (E) RT-PCR analysis of *BmprIB* mRNA isolated from the olfactory epithelium or limb of WT(+/+), *BmprIB*^{Tg} heterozygous (+/–) or *BmprIB*^{Tg} homozygous (–/–) mutants. Top and bottom panels, *BmprIB* cDNAs were synthesized from total RNA (1 μg) using primer R4, and amplified with two different sets of *BmprIB* region-specific primers: upper panel, F9 and R5 (exons 10-13); bottom panel, primers F2 and R14 (exons 1-5). The RT reaction was carried out in the presence (+RT, lanes 1-5) or absence (-RT, lanes 6-10) of reverse transcriptase. As expected given the deletion of exon 1 in the *BmprIB*^{Tg} allele, form 1 transcripts were not detectable in mutant samples (bottom panel). Form 2 transcripts could be detected in mutant olfactory epithelium, but not limb (upper panel). Middle panel, amplification products of alpha-4-tubulin (Freytag and Geddes, 1992) cDNAs synthesized from the same samples as above.

mRNA transcribed from one promoter, the two isoform classes reflect the evolution of two *BmprIB* gene promoters: one which is located at a distance and is required for expression in the developing limb skeleton (promoter 1), and one which is situated proximal to the coding region and drives expression in neural epithelium (promoter 2). Details of the promoter sequence will be presented elsewhere.

BmprIB^{Tg} is a regulatory allele, missing *cis*-sequences required for limb expression

In situ hybridization to *BmprIB*$^{Tg/Tg}$ embryos at 11.5-14.5 dpc showed only a subset of the wild-type *BmprIB* expression pattern. Most notable was the loss of *BmprIB* expression in the mesenchymal condensations of the developing limb (Fig. 3B) and vertebral column (Fig. 3D), indicating that the *BmprIB*^{Tg} allele is null with respect to the limb. These hybridization findings were confirmed by RT-PCR (Fig. 3E) using two different sets of *BmprIB* region-specific primers. Indeed, this lack of detectable *BmprIB* mRNA in mutant limb is consistent with the insertion mutation being a deletion of exon 1, which would preclude expression of the only *BmprIB* RNA species normally found in limb.

In contrast to the loss of transcription in mesenchyme, *BmprIB* mRNA was detectable in mutant olfactory epithelium (Fig. 3D,E, lane 1). 5′ RACE on dissected *BmprIB*$^{Tg/Tg}$ neuroepithelium identified form 2 transcripts only. This supports the notion that form 2 RNAs are transcribed off a promoter downstream from the 3′ end of the transgene-induced deletion.

While the insertion mutation abolishes *BmprIB* expression in discrete tissues, no new sites of expression were detected. It is therefore unlikely that the insertional mutation either introduces new regulatory elements driving ectopic IB expression or removes silencer elements that would normally mask expression. The *BmprIB* ^{Tg} allele is, therefore, a regulatory allele in which *cis*-sequences required for skeletal expression have been deleted.

Digit cartilage fails to develop in *BmprIB*^{Tg} mutants

Adult *BmprIB*$^{Tg/Tg}$ mice show loss of proximal and medial phalanges and fusion of sesamoid bones that normally articulate with these missing elements. Because the *BmprIB*^{Tg} allele is null with respect to the developing limb, these findings indicate that BMPRIB is required for the formation of endochondral-derived phalanges (P1 and P2). To analyze where in the process of phalangeal development IB signaling is required, we examined mutant limbs using both histological and molecular markers, asking if BMPRIB is essential for the early specification, proliferation, or condensation of prechondrogenic mesenchyme, or if IB is necessary for the later steps of chondrocyte proliferation and differentiation.

Each digit normally arises by sequential segmentation of a single chondrogenic condensation, the digital ray. This progressive process can be visualized histologically, using the general cartilage stain Alcian blue and, molecularly, using the cartilage differentiation markers *Collagen II* and *Indian Hedgehog (Ihh)*. Collagen II, encoded by the *Cola1(II)* gene is an early chondrocyte-specific marker (Lee et al., 1996). *Ihh*, which encodes a member of the Hedgehog family of signaling molecules, is initially expressed by a subset of chondrocytes residing in the interior of early condensations. As the condensation matures, *Ihh* expression becomes progressively restricted to postmitotic prehypertrophic chondrocytes (Bitgood and McMahon, 1995).

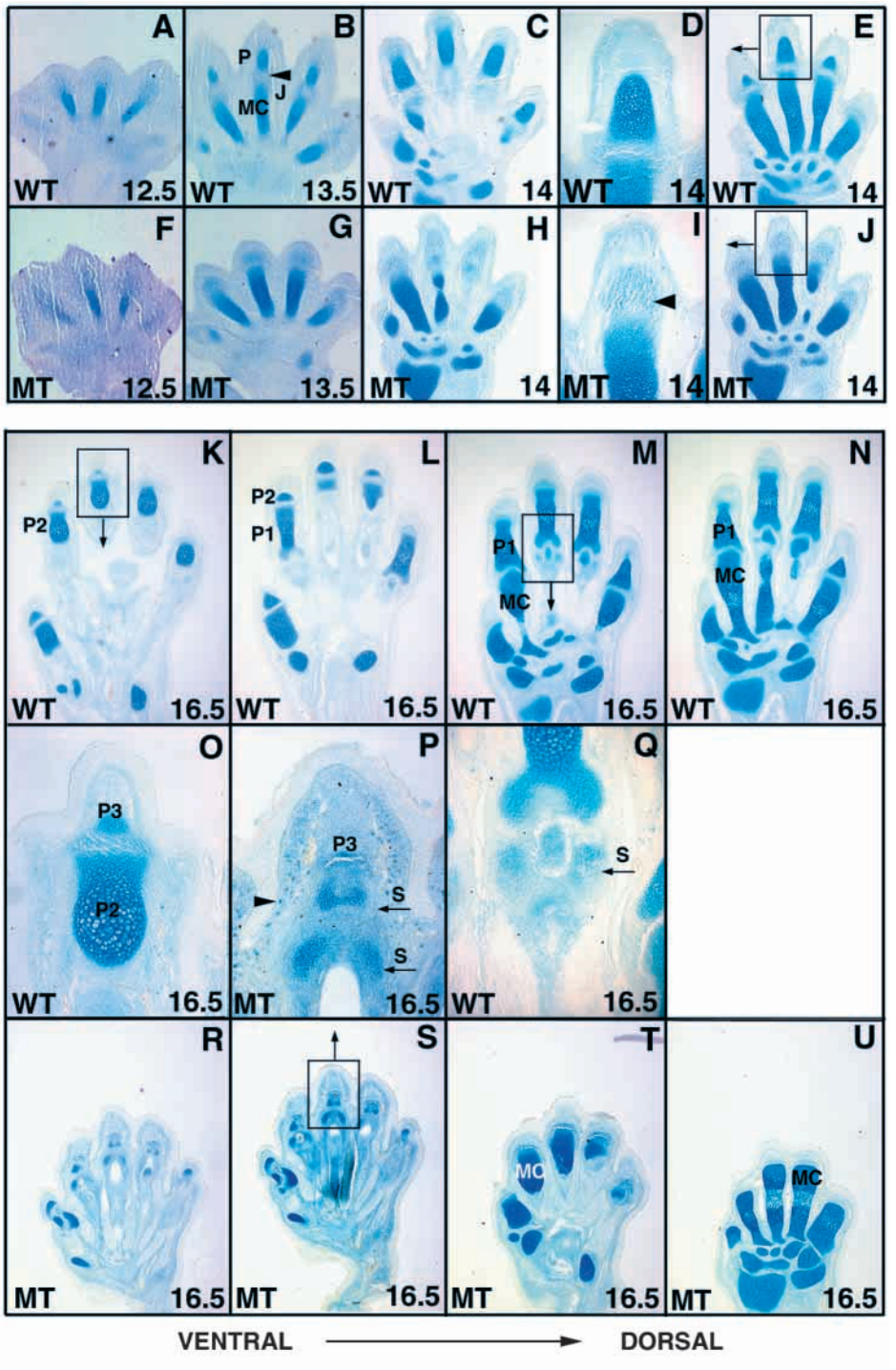

Fig. 4. BMPRIB is required to generate digit cartilages. Histologic analysis of cartilage formation in the *BmprIB*^{Tg} mutant. Sections of forelimbs from different stages of wild-type (A-E, K-N) and mutant (F-J, R-U) embryos were stained with Alcian blue to reveal cartilage. In all the panels, embryonic stage (dpc) is indicated in the lower right. (A-E) Segmentation of the WT digital ray to generate metacarpal (MC) and phalangeal (P) elements, separated by an Alcian blue-negative region marking the future joint (J) space (arrowhead). A more dorsal section of the limb shown in C is shown in E. (D) Higher magnification of digit 3 shown in E. (F-J) Segmentation fails to occur in *BmprIB*^{Tg} mutant digital rays. A more dorsal section of the limb in H is shown in J to confirm complete absence of phalanges. (I) Higher magnification of digit 3 shown in J. Note the halo of weakly staining mesenchyme surrounding the distal end of the metacarpal (arrowhead). (K-N) Segmentation in WT limbs at 16.5 dpc generates distinct proximal (P1) and medial (P2) elements. Sections progress from ventral, K, to dorsal, N. (O) Higher magnification of digit 3 shown in K. (Q) Higher magnification of metacarpophalangeal region of digit 3 shown in M. Note the forming metacarpophalangeal sesamoid cartilages (S, indicated by the arrow) that lie ventral to the actual metacarpal element which can be seen in the more dorsal section N. (R-U) Mutant limbs at 16.5 dpc show complete absence of P1 and P2 elements. Sections progress from ventral, R, to dorsal, U. (P) Higher magnification of digit 3 shown in S. Despite the lack of P1 and P2 elements, both metacarpophalangeal and distal sesamoids (S) develop, fusing across the midline (see arrows). Ectopic Alcian blue-positive cells are indicated by the arrowhead.

In the wild-type animal, cartilaginous digital rays are clearly apparent in both the forelimb and hindlimb by 12.5 dpc (Fig. 4A). As the digital ray elongates, it eventually reaches a size and stage where the more proximal region differentiates and expresses *Ihh*, while the distal domain continues to aggregate mesenchyme from the progress zone. The outcome, by 13.5 dpc, is segmentation of the ray into two subelements: a proximal metacarpal and a distal phalanx (Fig. 4B). While each subelement stains strongly with Alcian blue (Fig. 4B-E) and expresses high levels of *Collagen II* (Fig. 5A,B), the intervening joint region does not. Differentiation progresses with *Ihh* detectable in both the metacarpal elements (Fig. 6E) and phalanges (Fig. 6E,G). By 14.5 dpc the phalanx has elongated and started to cleave such that, by 16.5 dpc, distinct P1 and P2 subelements can be recognized (Fig. 4K-O).

Although *BmprIB*$^{Tg/Tg}$ and wild-type embryonic limbs are indistinguishable by Alcian blue staining at 12.5 dpc (Fig. 4A,F), a striking difference was observed by 13.5-14 dpc: mutant metacarpals (digital rays) failed to segment, despite being within a normal size range and expressing wild-type levels of *Collagen II* (Fig. 5C,D) and *Ihh* (Fig. 6F,H). A halo of mesenchyme surrounds the distal end of each mutant metacarpal giving the appearance of prechondrogenic cells attempting to condense and differentiate (Fig. 4H-J). This halo stained weakly with Alcian blue, but was negative for Collagen II, except for an outerzone of cells suggestive of perichondrium

(Fig. 5C, arrowhead). Analysis of hindlimbs showed similar findings. Despite the lack of P1 and P2 elements in *BmprIB*$^{Tg/Tg}$ mutant limbs, sesamoid cartilages can be observed at 16.5 dpc (Fig. 4P,S). In contrast to wild type (Fig. 4Q), mutant sesamoid cartilages appear to be fusing at the midline (Fig. 4P,S), consistent with the adult sesamoid phenotype. Overall, no ectopic structures such as webbing were observed, as might be expected if the digit mesenchyme were reallocated. Interestingly, individual Alcian blue-positive cells were found dispersed throughout the most distal mesenchyme of mutant 16.5 dpc forefeet and hindfeet (Fig. 4P, arrowhead). The exact nature and source of these cells is unclear, but our analysis suggests that, as the metacarpals elongate and the sesamoid and P3 phalangeal cartilages develop, the Alcian blue-positive cells in the halo observed at 14.5 dpc get displaced laterally and distally. Thus, in the absence of BMPRIB, prechondrogenic limb mesenchyme is specified to form digital rays that differentiate normally at the proximal ends, but which fail to undergo digit morphogenesis distally.

Feedback regulation of *Gdf5, Gli2* and *Gli3* is disrupted in *BmprIB*^{Tg} mutants

Since the failure to form digits appeared to be linked in *BmprIB*$^{Tg/Tg}$ mutants to a defect in segmentation, we examined molecular markers for joint development, including the TGFβ family member, *Gdf5* (Storm et al., 1994), and two putative zinc finger transcription factors, *Gli2* and *Gli3* (Hui et al., 1994). Expression of *Gdf5* has been reported to identify a mesenchyme domain of approximately 30-35 cell diameters distal to the growing 12.5 dpc digit ray (Storm and Kingsley, 1999); these marked cells appear specified to go on to condense and form cartilage. 24 hours later, expression is restricted to a domain of approximately 15-20 cell diameters in the region of the presumptive metatarsophalangeal joint. By 14.5 dpc, this domain further restricts to a narrow band marking the metacarpophalangeal articulation. *Gli2* and *Gli3* are expressed in a similar profile (Hui et al., 1994; Storm and Kingsley, 1999) and are considered, along with *Gdf5*, to first mark prechondrogenic mesenchyme and, later, mark joint interzones.

Analyses of IB mutant limbs showed expanded expression domains for *Gdf5, Gli2* and *Gli3* (Fig. 6L,N,P). Expression remained broad in the mutant even at 13.5 dpc, and failed to restrict to the presumptive metacarpophalangeal joint (Fig. 6K, arrowhead in wild-type limb). Thus, in the absence of IB function, there is an expansion of *Gdf5, Gli2* and *Gli3* to include nearly all distal mesenchyme. These observations suggest that prechondrogenic mesenchyme is present in the phalangeal region but that it fails to mature to form the P1/P2 anlagen. One explanation is that BMPRIB directs the differentiation of prechondrogenic mesenchymal cells into chondrocytes and is therefore necessary for further digit morphogenesis. In part, chondrocyte differentiation requires a threshold density of cells (Takahashi et al., 1998); the failure to form digits could therefore also reflect a defect in the condensation or proliferation process.

A similar expansion of *Gdf5* and *Gli3* expression is reported in mice homozygous for the frameshift null allele *Gdf5*$^{bp\text{-}J}$. This molecular phenocopy lends further support to the idea that GDF5 and BMPRIB may participate in common or parallel pathways in vivo, and that one common outcome is downregulation of *Gdf5, Gli2* and *Gli3*.

BmprIB is required for *Ihh* and *Gli1* expression in the phalangeal region

Gli1 expression is initially found throughout the condensing digit ray; however, rather than becoming restricted to the presumptive joint interzone like *Gli2* and *Gli3*, *Gli1* mRNA localizes to the perichondrium (Hui et al., 1994; Fig. 6I). In *BmprIB*$^{Tg/Tg}$ mutant limbs, *Gli1* transcripts are undetectable in the presumptive P1/P2 region (Fig. 6J), this is in contrast to the expanded domains of *Gli2* and *Gli3* (Fig. 6N,P). As described above, *collagen II* and *Ihh* RNA are similarly absent in the phalangeal region. Loss of these chondrocyte markers in the digital region of *BmprIB*$^{Tg/Tg}$ mice, together with persistence of prechondrogenic markers (*Gdf5, Gli2* and *Gli3)*, indicates that BMPRIB signaling is required for advancing from the prechondrogenic to the chondrogenic stage in digit formation.

Gli1 has been shown to be a target of Sonic hedgehog (Shh) signaling in the early limb bud (Hynes et al., 1997; Lee et al., 1997; Marigo et al., 1996). The coordinate loss of both *Ihh* and *Gli1* in the phalangeal region of *BmprIB*$^{Tg/Tg}$ limbs suggests that in this later setting in the distal limb, *Gli1* is likely to be a physiologic target of Indian hedgehog signaling.

Reduced mesenchymal cell proliferation in mutant phalangeal region followed by excessive apoptosis

To assess whether lack of cartilage differentiation in the phalangeal region of *BmprIB*$^{Tg/Tg}$ mice involves a defect in cell proliferation, we analyzed bromodeoxyuridine (BrdU) incorporation into both early progress zone mesenchymal cells (11.5-12.5 dpc) and into later chondrogenic cells in the phalangeal regions (13.5-14.5 dpc). Though no differences were observed between mutant and wild-type at 11.5 and 12.5 dpc (Fig. 7A-D), we did detect a 6.4-fold reduction in the percentage of BrdU-positive nuclei in the digital region of mutant limbs at 13.5 dpc (P<0.005, Student's t-test) (Fig. 7E,F). BMPRIB signaling is, therefore, not essential to maintain the high rate of proliferation observed in the early progress zone mesenchyme, but is required for proliferation of later prechondrogenic cells in the digit region.

In addition to exhibiting a decrease in cell proliferation rates, the mutant digit mesenchyme at 13.5 -14.5 dpc failed to condense and organize into tightly packed chondrocytes. Two morphological indicators of this differentiation process include the flattening of outerzone (preperichondrial) cells into concentric layers, and longitudinal stacking of inner zone (chondrogenic) cells. Both of these morphologic changes failed to occur in mutant digits (Fig. 7F,H).

By 14.5 dpc, mutant digital mesenchyme becomes even more disorganized, characterized by pyknotic cells and empty spaces starting at the presumptive metacarpophalangeal joint and extending well into the prechondrogenic aggregation. Because these changes in tissue integrity were suggestive of cell death, we analyzed mutant limbs for signs of apoptosis. Both wild-type and *BmprIB*$^{Tg/Tg}$ limbs at 11.5 and 12.5 dpc showed a low incidence of cell death in the progress zone, as assessed by end labeling of fragment DNA (data not shown). Normal levels of apoptosis were, however, observed in interdigital mesenchyme of both mutant and wild-type embryos, indicating that the apoptotic process has not been more generally disrupted in the mutant. Together with the BrdU analysis, these results suggest that the supply of progress zone mesenchyme is normal in *BmprIB*$^{Tg/Tg}$ limbs, arguing

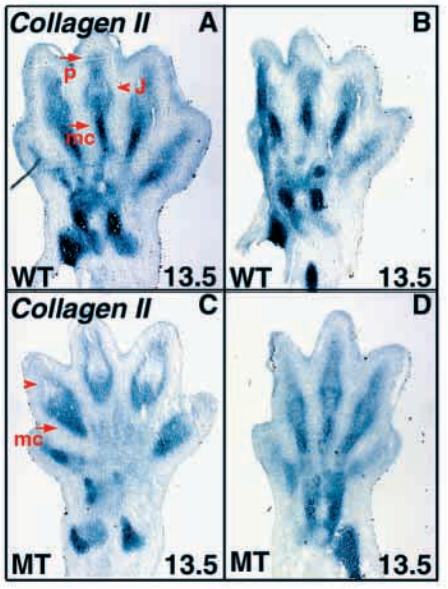

Fig. 5. BMPRIB is required for *Collagen II* expression in the phalangeal region. Near adjacent sections from WT (A,B) and *BmprIB*^{Tg} mutant (C,D) hindlimbs at 13.5 dpc were hybridized with a probe to *Collagen II*. (A,B) Both metacarpal (MC) and phalangeal (P) elements express *Collagen II*, while the future joint space (J) does not. (C,D) Note the phalangeal region fails to express Collagen II, except for an outerzone of perchondrial-like cells (arrowhead).

against insufficient starting mesenchyme as causing the reduction in phalangeal elements.

In contrast to the normal appearing early stage limbs, later stage mutant limbs (13.5 and 14.5 dpc) show an approximate 5-fold increase in cell death as compared to wild-type limbs (P<0.005, Student's t-test) (Fig. 8). The apoptotic area corresponds to the presumptive metacarpophalangeal joint space and extends distally over time to include most of the disorganized digit mesenchyme. Interestingly, this region of excessive cell death corresponds to the expanded expression domains of *Gdf5*, *Gli2* and *Gli3*. Because expression of this gene set goes from marking prechondrogenic mesenchyme at early stages, to marking joints at later stages and because joint formation is associated with programmed cell death, it is possible that expanded joint development contributes to the brachydactyly phenotype. In summary, BMPRIB appears required to condense prechondrogenic digit mesenchyme into a proliferating cartilage focus. In the absence of this chondrogenic program and in the presence of prolonged expression of *Gdf5*, *Gli2* and *Gli3*, excessive cell death occurs. The end result is complete loss of endochondral-derived phalanges.

BmprIB^{Tg}*; Gdf5*$^{bp\text{-}J}$ double mutants indicate that GDF5 interacts with BMPRIB in vivo

GDF5 is likely to signal, at least in part, through BMPRIB. This is based on the observations that *BmprIB*^{Tg} and *Gdf5*$^{bp\text{-}J}$ homozygotes each show a similar loss of phalanges

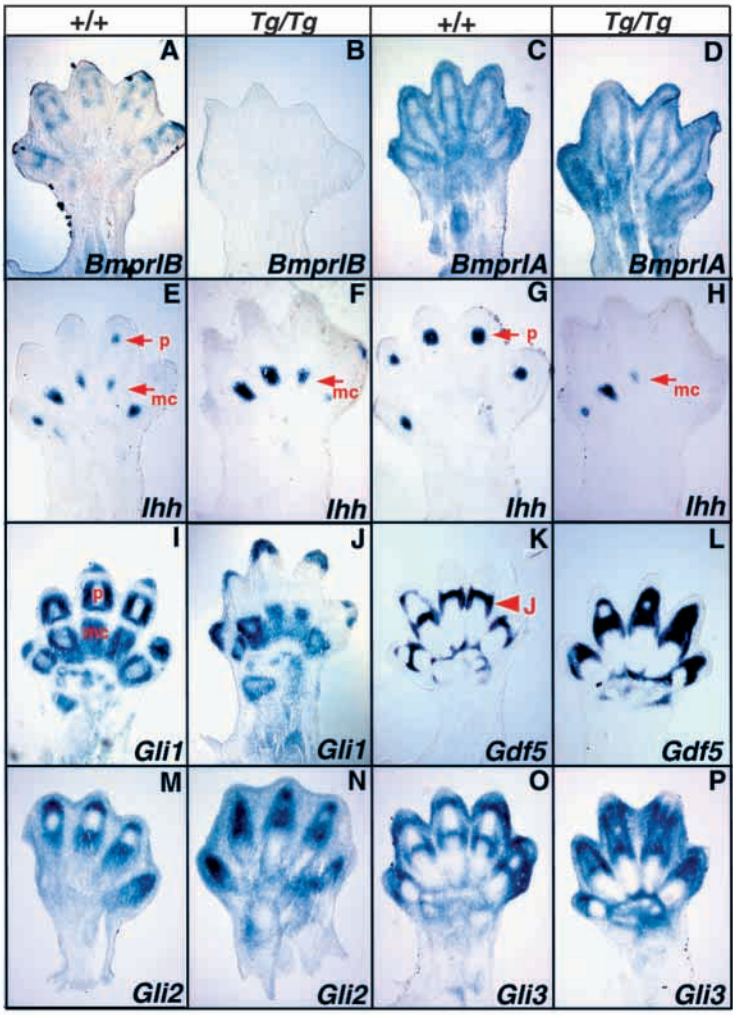

Fig. 6. Gene expression patterns suggest that BMPRIB signals differentiation of prechondrogenic digit mesenchyme. Sections of forelimbs from wild-type (A,C,E,G,I,K,M,O) and *BmprIB*^{Tg} mutant (B,D,F,H,J,L,N,P) embryos at 13.5 dpc were hybridized with probes to *BmprIB* (A,B), *BmprIA* (C,D), *Ihh* (E-H), *Gli1* (I,J), *Gdf5* (K,L), *Gli2* (M,N), and *Gli3* (O,P). (A,B) *BmprIB* expression in wild-type (A) and *BmprIB*^{Tg} mutant (B) forelimbs. No *BmprIB* expression was detected in the mutant limb. (C,D) *BmprIA* expression in wild-type (C) and *BmprIB*^{Tg} mutant (D) forelimbs. No differences in expression were detected. (E-H) *Ihh* expression in wild-type (E,G) and mutant (F,H) forelimbs. *Ihh* is expressed in an inner set of cells in both the metacarpals(mc) and phalanges(p). The more ventral wild-type section (G) documents the full extent of *Ihh* expression in the developing phalanges. While mutant limbs (F,H) express *Ihh* in the developing metacarpals, no transcripts could be detected in the phalangeal regions. (I,J) *Gli1* expression in wild-type (I) and mutant (J) limbs. In the mutant, perichondrial expression normal to this stage, is missing in the phalangeal region. (K,L) *Gdf5* expression in wild-type (K) and mutant (L) limbs. At this stage, *Gdf5* is expressed in the presumptive joint interzones (K). The metacarpophalangeal joint region is indicated by an arrowhead. In the mutant (L), *Gdf5* expression is much broader, extending distally into the phalangeal region. (M,N) *Gli2* expression in wild-type (M) and mutant (N) forelimbs. (O,P) *Gli3* expression in wild-type (O) and mutant (P) forelimbs. Like *Gdf5*, both *Gli2* and *Gli3* expression is broadened in the mutant.

(Gruneberg and Lee, 1973; Storm et al., 1994; and reported here), and because in vitro studies show high-affinity binding of GDF5 to BMPRIB as compared to other type I receptors

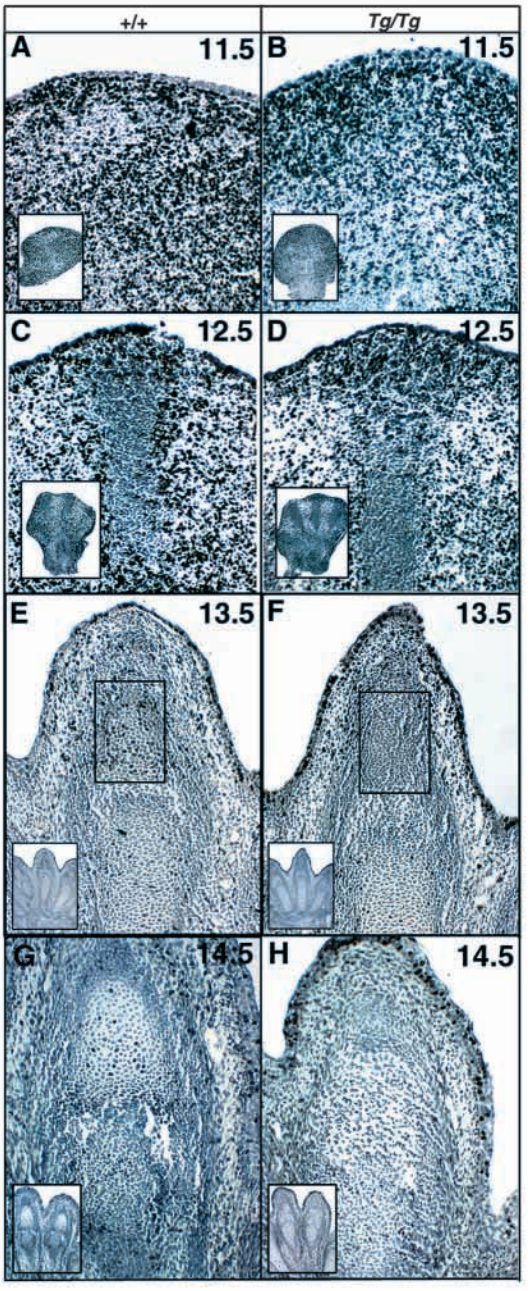

Fig. 7. Reduced cell proliferation in the digit region of *BmprIB*^{Tg} mutants. (A-H) BrdU labeling in the forelimb of wild-type (A,C,E,G) and *BmprIB*^{Tg} mutant (B,D,F,H) embryos. Developmental stages in dpc are indicated in the upper right corner of each panel. Insets in lower left corners show a low magnification view of the forelimb. BrdU-positive nuclei are stained black. All nuclei are weakly counterstained with hematoxylin. At 13.5 dpc, mutant limbs (F) showed a 6.4-fold reduction in the percentage of BrdU-positive nuclei in the bracketed digit region (WT, 19.8±5.2% s.d.; *BmprIB*^{Tg} mutant, 3.1±1.8% s.d.; $P<0.005$, Student's *t*-test). (G,H) At 14.5 dpc, mutant digit mesenchyme has failed to condense and organize into tighly packed chrondrocytes. Note that the mutant digit mesenchyme is comprised of pyknotic cells and empty spaces.

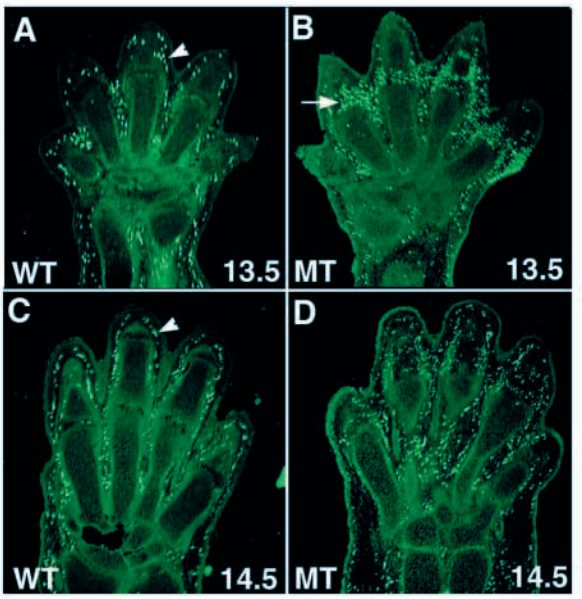

Fig. 8. Excessive cell death in the digit region of *BmprIB*^{Tg} mutants. Sections of 13.5 dpc (A,B) and 14.5 dpc (C,D) forelimbs showing apoptotic cells, detected by end labeling of fragmented DNA. In wild-type (WT) embryos (A,C), a few apoptotic cells are detected in the joint and interdigital regions. Background fluorescence necklacing each digit reflects blood cells (arrowheads in A,C). Mutant limbs at 13.5 dpc showed a 5-fold increase in apoptotic cells at the presumptive metacarpophalangeal joint (B, arrow) (WT, 2.0±1.1% s.d.; *BmprIB*^{Tg} mutant, 9.6±2.6% s.d.; $P<0.005$, Student's *t*-test). By 14.5 dpc, apoptotic cells can be seen thoughout the digital region.

(Nishitoh et al., 1996). To investigate whether BMPRIB indeed transduces GDF5 signals in vivo, we compared skeletons isolated from adult *BmprIB*^{Tg}*; Gdf5*$^{bp\text{-}J}$ double mutants, single mutants and compound heterozygotes. Skeletal preparations are shown in Fig. 9 alongside schematics illustrating the observed digit defects.

As described earlier, *BmprIB*^{Tg} homozygotes display normal or slightly shortened metatarsals, each articulating directly with a terminal P3 phalanx; P1 and P2 phalanges are absent. *Gdf5*$^{bp\text{-}J}$ homozygotes show metatarsals that are markedly reduced in length, and loss of the digital-ray-derived phalanges P1 and P2; in place, is a rudimentary phalanx thought to be derived by appositional cartilage growth from perichondrial-like mesenchyme (Storm and Kingsley, 1999). In the digital region, *BmprIB*^{Tg}*; Gdf5*$^{bp\text{-}J}$ double mutants appear similar to *Gdf5*$^{bp\text{-}J}$ single mutants, indicating that GDF5 signals digit cartilage condensation and proliferation through BMPRIB. While normal digit cartilages failed to development in the double mutant, runted phalangeal elements, similar to those found in *Gdf5*$^{bp\text{-}J}$ single mutants were observed (Fig. 9D,H). In contrast to the digit region, synergistic malformations were found in the carpal and tarsal bones of double mutants: individual metacarpals (metatarsals) failed to segment properly from the carpal (tarsal) bones. This defect was especially striking in the hindfoot, between metatarsal III, cuneiform III and the navicular bone (Fig. 9, arrowhead). This synergistic phenotype indicates that BMPRIB and GDF5 serve redundant functions in regulating segmentation of the digital arch.

It is possible that some differences in cartilage growth

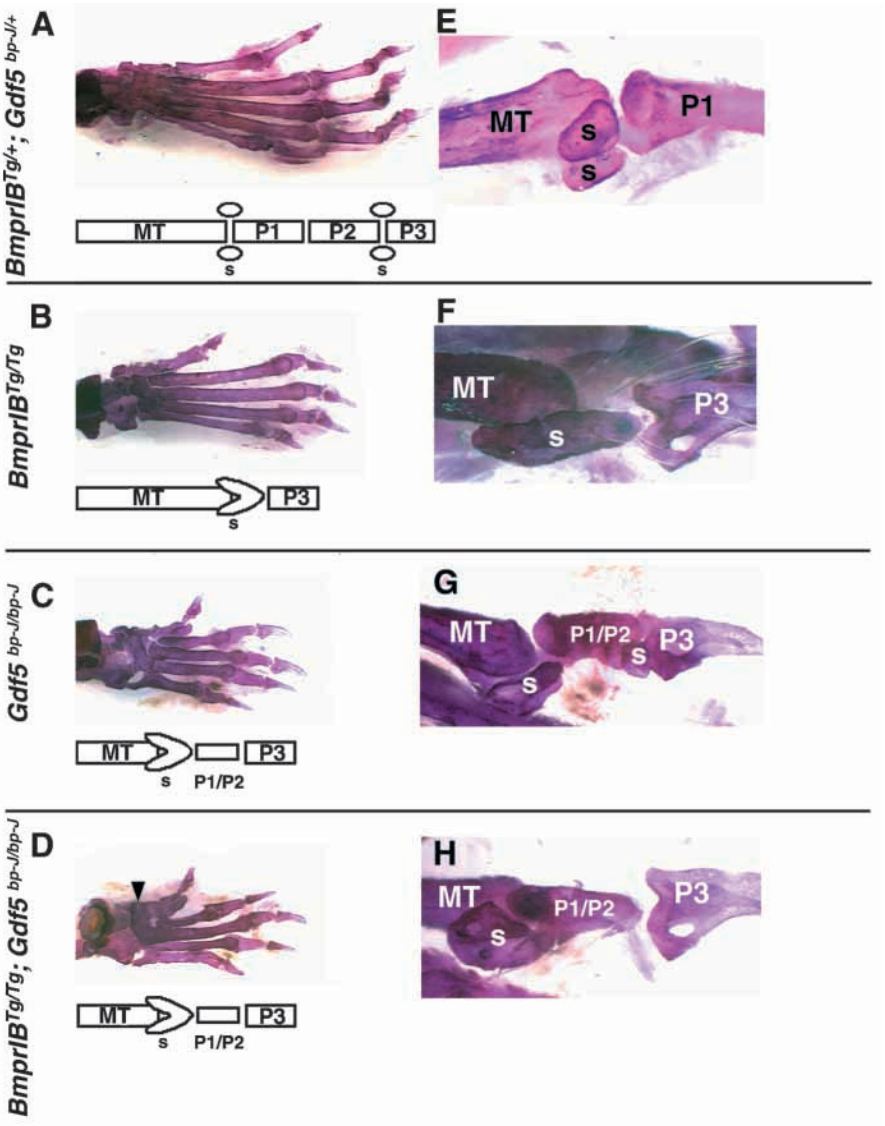

Fig. 9. *BmprIB* and *Gdf5* interact genetically. Adult hindfeet stained with Alizarin red. In each panel, the metatarsal (MT) and phalangeal (P1-P3) bones in a given digit ray are diagrammed as a ventral view below. (A) Dorsal view of a $BmprIB^{Tg/+}$; $Gdf5^{bp\text{-}J/+}$ compound heterozygous hindfoot. (E) Higher magnification, lateral view of the metatarsophalangeal joint (dorsal is at the top). Note the paired sesamoid cartilages (s). (B,F) Dorsal view of a $BmprIB^{Tg/Tg}$ homozygous mutant hindfoot. Note that the metatarsals are of normal size but the P1 and P2 phalanges are missing, and the sesamoid cartilages are fused. (F) Higher magnification lateral view (magnification as per E) showing the novel articulation between the metatarsal, the abnormal sesamoid, and the terminal P3 phalanx. (C,G) Dorsal view of a $Gdf5^{bp\text{-}J/bp\text{-}J}$ homozygous mutant hindfoot. The metatarsals are significantly shortened, and rudimentary phalanges (P1/P2) replace the normal P1 and P2 elements. Sesamoids are also fused. (G) Higher magnification lateral view (magnification as per E). (D,H) Dorsal view of a $BmprIB^{Tg/Tg}$; $Gdf5^{bp\text{-}J/bp\text{-}J}$ double mutant hindfoot. Note that the metarsals are of similar length to those displayed by $Gdf5^{bp\text{-}J/bp\text{-}J}$ single mutants. Unlike $BmprIB^{Tg/Tg}$ single mutants, the double mutant does generate rudimentary P1/P2 phalanges. (H) Higher magnification lateral view (magnification as per E).

observed between $BmprIB^{Tg}$ and $Gdf5^{bp\text{-}J}$ mutant mice could, in part, stem from differences in the genetic background of the mutants: B6SJL for $BmprIB^{Tg}$ versus AJ for $Gdf5^{bp\text{-}J}$. This is unlikely given that fully penetrant brachydactyly has been observed in IB mutants developed on other genetic backgrounds (129/Sv and a mixed 129/Sv × C57Bl/6; Yi, 2000), suggesting that the brachydactyly phenotype is not readily altered by strain-specific modifier genes.

DISCUSSION

We have shown that $BmprIB^{Tg}$ mutants display a complete loss of endochondral-derived phalanges. Our analyses indicate that BMPRIB plays multiple roles in development of the distal limb skeleton; these include signaling cartilage condensation and differentiation from the digital blastema and regulating cartilage segmentation to yield subelements. In addition, we have further delineated GDF5 function in vivo, finding that GDF5 signals digit cartilage formation through IB, but regulates the overall length of skeletal elements largely through alternative receptors. These studies, in conjunction with previous analyses of *Gdf5* null mice (Storm et al., 1994; Storm and Kingsley, 1999), indicate that IB and GDF5, acting together and separately, play pivotal roles in determining distal limb structure.

In addition to delineating IB and GDF5 function in skeletal development, we have also determined the structure of the *BmprIB* gene and have identified two promoters, one of which is responsible for expanding *BmprIB* expression into the developing limb. Acquisition of this promoter may have implications for the evolutionary innovation of digits in the distal limb, and its utilization may contribute to the species-to-species variability found in distal limb architecture.

BMPRIB is essential for differentiation of digit cartilage

Previous misexpression studies performed in the chick (Kawakami et al., 1996; Zou et al., 1997; Merino et al., 1998) suggest that BMPrIB may act as a direct effector of chondrogenesis, consistent with its presence in cartilage primordia. In addition to promoting cartilage formation, a constitutively active IB receptor (caBMPrIB) has also been shown capable of inducing interdigital cell death (Zou et al., 1997). This latter result, however, is at odds with the absence of detectable *BmprIB* mRNA in interdigital tissue (this report, Fig. 6A; see also Zou et al., 1997). Should IB serve both chondrogenic and apoptotic functions, then a IB null mutation

would be predicted to result in a reduction in distal cartilage elements with a concomitant increase in interdigital tissue. Our analysis of *BmprIB*^{Tg} mutants shows that digit cartilages are lost without concomitant webbing; this finding supports the idea that IB signals chondrogenesis and argues against a physiological role for IB in signaling cell death.

Because distal pattern appeared to be specified in *BmprIB*$^{Tg/Tg}$ mutant limbs (operationally defined by the early expression of the prechondrogenic markers *Gdf5, Gli2* and *Gli3),* we propose that the major function of IB is to signal condensation and differentiation of prechondrogenic cells, without which further digit morphogenesis cannot occur. It is, of course, possible that, in the absence of normal cartilage condensation and differentiation, additional IB functions go unrealized and, therefore, cannot be excluded (e.g. maintenance of the differentiated phenotype).

While *BmprIB* expression is lost from a number of developing tissues in *BmprIB*$^{Tg/Tg}$ embryos (vertebral condensations, gut, kidney and urogenital tract), the observed defects are restricted to distal limb (reported here) and distal genitals (to be described elsewhere). One explanation for the circumscribed phenotype is that other type I receptors can substitute for the loss of IB in these tissues. Such compensatory mechanisms are either insufficient or do not exist in distal limb and genitals, or are compromised by the accompanying misregulation of *Gdf5*.

BMPRIB interacts genetically with GDF5

Previous in vitro experiments showed that GDF5 could bind to different sets of type I receptors and that binding was most efficient to BMPRIB. Moreover, in cell culture, IB was shown to transduce a transcriptional activation signal following stimulation with GDF5 (Nishitoh et al., 1996). Examination of *BmprIB*^{Tg}; *Gdf5*$^{bp\text{-}J}$ double mutants indicates that, in vivo, BMPRIB does indeed mediate signals for GDF5, the outcome being formation of digit cartilage. Consistent with this genetic interaction, is our finding that BMPRIB, like GDF5 (Storm and Kingsley, 1999), is required to downregulate *Gdf5, Gli2* and *Gli3* expression in the digit/joint region, but not in perichondrium. The phenotypic consequence of GDF5 signaling in these two regions (digit/joint versus perichondrium) is therefore different, suggesting that GDF5 may signal through distinct receptor complexes or trigger different downstream intracellular pathways depending on the spatial location.

Micromass limb cultures show that GDF5 can modulate the initial stages of chondrogenesis by increasing cell adhesion within a mesenchymal condensation (Francis-West et al., 1999; Hotten et al., 1996). Interestingly, prechondrogenic digit mesenchyme in *BmprIB*$^{Tg/Tg}$ limbs appears unable to condense and organize into a cartilage element. Given this block in progressing from loosely aggregated prechondrogenic cells to compact chondroblasts, we propose that the physiological outcome of GDF5/BMPRIB signaling in the early digital ray is an increase in cell adhesion. The resultant condensation and high cell density then enables further cartilage proliferation and differentiation.

Distinct and redundant roles for BMPRIB and GDF5 suggest combinatorial signaling in vivo

While both *BmprIB*^{Tg} and *Gdf5*$^{bp\text{-}J}$ single mutants exhibit loss of endochondral-derived phalanges, the skeletons are nonetheless readily distinguishable due to a striking difference in bone length. *BmprIB*^{Tg} mutant limbs display near normal bone length, while *Gdf5*$^{bp\text{-}J}$ limbs are significantly shortened (Gruneberg and Lee, 1973; Storm et al., 1994). Double mutants show no further reduction. Thus, in contrast to GDF5, IB is not required to sustain normal longitudinal growth of more proximal limb elements.

The reciprocal phenotype of an increase in bone length has been reported following overexpression of *Gdf5* in the chick limb (Francis-West et al., 1999; Merino et al., 1999). This has been interpreted within the context of the endogenous *Gdf5* expression profile to suggest an additional role for GDF5. First, when *Gdf5* is expressed in prechondrogenic cells, it promotes condensation by increasing cell adhesion. Later, when its expression is restricted to joints, it may signal to the epiphyses of adjacent skeletal elements to control chondrocyte proliferation and therefore overall bone length (Francis-West et al., 1999). Although IB is expressed in the developing cartilage epiphyses and has been hypothesized to signal chondrocyte proliferation, our loss-of-function analyses show that IB is not required to achieve normal bone length once the initial condensation has been established. This raises the possibility that, early on, GDF5 signals mesenchymal condensation through IB but, later, signals chondrocyte proliferation through additional type I receptors.

Although major differences in bone length were not observed between *BmprIB*$^{Tg;}$ *Gdf5*$^{bp\text{-}J}$ double mutants and *Gdf5*$^{bp\text{-}J}$ single mutants, synergistic malformations were found in the carpal and tarsal bones of double mutants. BMPRIB and GDF5 therefore serve redundant functions in regulating segmentation of the digital arch, with IB mediating segmentation signals from other GDF/BMP ligands and GDF5 activating other receptors. Moreover, this analysis has revealed a function for BMPRIB in cartilage segmentation that was not uncovered through study of single mutants.

Overexpression of *Gdf5* in *BmprIB*^{Tg} mutants correlates with apoptosis

The complete loss of P1 and P2 phalanges in *BmprIB*^{Tg} homozygotes would, at first glance, suggest that BMPRIB is required for development of digit cartilages, playing a role in two processes: the condensation and differentiation of digit cartilage from the digital ray, and the appositional growth of cartilage from perichondrium. In contrast, GDF5 appears to be required for the development of digit cartilage from the digital ray, but is nonessential for appositional-like growth (as rudimentary P1/P2 elements do develop). This would suggest that a different GDF or BMP signals appositional growth through IB. Surprisingly, rudimentary phalanges were found in the double mutant, suggesting that neither BMPRIB nor GDF5 are required for appositional growth. This seemingly contradictory finding makes sense when consideration is given to the genes that we see affected in *BmprIB*^{Tg} homozygotes.

Although the primary defect in *BmprIB*^{Tg} homozygotes is loss of *BmprIB* expression in the limb, this loss is accompanied by expanded and prolonged expression of *Gdf5, Gli2* and *Gli3* in the digital region (Fig. 6). The complete failure to develop digit cartilage in *BmprIB*^{Tg} homozygotes therefore results from the combined effects of both genetic alterations: loss of *IB* and gain of *Gdf5, Gli2* and *Gli3*. The initial developmental defect in *BmprIB*^{Tg} homozygotes (observed at 13.5 dpc) appears to

be a failure to condense and differentiate prechondrogenic cells into digit chondroblasts. In the absence of this IB-dependent differentiation step, prechondrogenic mesenchyme undergoes apoptosis in the region in which *Gdf5*, *Gli2* and *Gli3* are overexpressed. This tissue loss (readily apparent by 14.5 dpc; Figs 7H, 8) precludes later cartilage development through appositional mechanisms. Within this context, the simplest interpretation of the double mutant phenotype is that, in the absence of functional GDF5, the excessive apoptosis seen in $BmprIB^{Tg}$ single mutants does not occur, thereby allowing rudimentary phalanges to form by apposition. From this, we deduce that GDF5 signals the aberrant cell death observed in $BmprIB^{Tg}$ single mutants. Thus, the brachydactyly observed in $BmprIB^{Tg}$ limbs likely results from the combined effects of loss of IB (failure to condense and differentiate digit cartilage) and overexpression of *Gdf5* (later apoptotic loss of prechondrogenic mesenchyme).

Because the apoptosis observed in $BmprIB^{Tg}$ single mutant digits begins at the metacarpophalangeal joint and then extends distally, following the expanded *Gdf5* expression domain, we propose that GDF5 may signal the programmed cell death intrinsic to digit segmentation and joint formation; indeed, this would be consistent with one of the putative functions for GDF5 put forth by Storm and Kingsley (1999). In our model, GDF5 would signal apoptosis through an alterative type I receptor, as the observed cell death occurred in the absence of BMPRIB. In the chick (Francis-West et al., 1999; Hotten et al., 1996; Merino et al., 1999) and in mouse limb culture (Storm and Kingsley, 1999), exogenous GDF5 protein has been shown to stimulate ectopic cartilage development, but not ectopic subdivisions in skeletal elements. Consequently, GDF5 would be necessary but not sufficient to induce cell death and joint formation. It is also possible that the cell death observed in $BmprIB^{Tg}$ single mutants results from abnormally high levels of GDF5 protein inappropriately activating (or even antagonizing) other type I receptors.

Together, the above genetic studies suggest a number of important conclusions regarding BMP signaling and skeletal development: (1) GDF5 signals digit formation through BMPRIB but regulates element length through an alternative type I receptor, (2) GDF5 and IB each exert segmentation functions, but, at least in part, do so independently, and (3) appositional cartilage growth is likely induced by other BMPs and receptors, since it occurs independent of both GDF5 and IB. Our analyses, not only identify both distinct and redundant functions for BMPRIB and GDF5 in skeletal development, but provide evidence that combinatorial BMP signaling occurs in vivo.

BMPRIB signaling and Gli proteins

In addition to regulating *Gdf5* expression, we show that BMPRIB activity is necessary to downregulate *Gli2* and *Gli3*, and is required for subsequent *Ihh* and *Gli1* expression. The $BmprIB^{Tg}$ mutation therefore genetically separates the activities of *Gli2* and *Gli3* from *Gli1*, consistent with gene inactivation experiments showing that Gli2 and Gli3 serve redundant functions during skeletal development (Mo et al., 1997). This in vivo distinction supports recent in vitro structure-function studies that divide the Gli proteins into two categories: Gli1 appears to function primarily as a transcriptional activator and primary mediator of Hh function; conversely, Gli2 and Gli3 exhibit strong repressor activity, antagonizing both Hh and Gli1 function (Ruiz i Altaba, 1999; Sasaki et al., 1999). Indeed, *Ihh* and *Gli1* are coordinately lost in the $BmprIB^{Tg/Tg}$ mutant limb suggesting that Gli1 is a physiologic target of Ihh signaling.

Genetic and biochemical studies have suggested that Gli proteins interact with the BMP-triggered signaling cascade. In vitro studies show that carboxy-terminally truncated Gli3 proteins (but not Gli1) complex with Smad proteins, and that the complexes are disrupted by BMP signaling (Liu et al., 1998). Moreover, genetic studies in mice suggest an interaction between BMP4 and Gli3 (Dunn et al., 1997), and human syndromes associated with Gli3 mutations, such as Pallister-Hall syndrome (Kang et al., 1997) and polydactyly type A (Radhakrishna et al., 1997), each display skeletal defects similar to those resulting from aberrant BMP signaling. Here we show that *Gli3* expression is downregulated by IB. Thus, BMPRIB signaling likely regulates Gli3 activity at two levels: by altering Gli3-Smad protein complexes and by regulating Gli3 transcription.

Use of an alternative distal promoter expands *BmprIB* expression into the developing limb

Our analyses of the *BmprIB* gene structure and mRNA isoforms in wild-type and mutant mice have identified a second, more distal promoter required for expressing *BmprIB* in the developing limb skeleton. Because expression of IB is uniquely required for digit formation, acquisition of this novel *cis*-regulatory region could represent a pivotal genetic step for driving morphological diversity in distal extremities, exemplified by the formation of digits during the fin to limb transition. A primary example of evolutionary recruitment of gene function to generate new distal limb structure, comes from the identification of a digit regulatory element driving expression of *Hoxd-10, Hoxd-11, Hoxd-12* and *Hoxd-13* in the autopod (van der Hoeven et al., 1996). Given the functional equivalence of many of the *Hox* gene products, it has been proposed that novel morphogenetic variants can arise only through major regulatory changes such as this global digit enhancer (Zakany and Duboule, 1999). Given the overlapping activities reported for the different type I BMP receptors, the same logic could hold here: generation of phalanges requires acquisition of novel *cis*-regulatory elements to expand type I receptor expression into the distal limb. This parallel between *BmprIB* and *Hox* gene regulation extends into the development of the distal urogenital tract. The same regulatory element that promotes *Hox* gene expression in digits, simultaneously promotes expression in the genital tubercle (van der Hoeven et al., 1996). Similarly, the same cis-regulatory region required to express *BmprIB* in the limb also drives expression in mesenchyme of the tubercle. Moreover, $Hoxa13^{+/-}$; $Hoxd13^{-/-}$ compound mutants display improper separation of the vagina from the urogenital sinus (Warot et al., 1997); although incompletely penetrant, $BmprIB^{Tg}$ mutants show a defect in vaginal development (S. T. B. and S. M. D., unpublished data) in addition to the fully penetrant brachydactyly described here. As put forth for the *Hoxd* genes, perhaps acquisition of this distal *BmprIB cis*-regulatory region has, in part, simultaneously shaped both the distal limb and distal genital tract.

We thank all those who supplied probes; Drs. Henry Kronenberg, Andrew McMahon, Ernestina Schipani, and Cliff Tabin for stimulating discussion; Dr Cliff Tabin for critical comments on the manuscript; and Jason Comander for BAC DNA sequence analyses. Work in S. M. D.'s laboratory was supported by grants from the National Institutes of Health, the John Merck Fund, the Rita Allen Foundation, and the Armenise-Harvard Foundation. S. B. is supported by a National Institutes of Health training grant.

REFERENCES

Astrom, A.-K., Jin, D., Imamura, T., Roijer, E., Rosenzweig, B., Miyazono, K., ten Dijke, P. and Stenman, G. (1999). Chromosomal localization of three human genes encoding bone morphogenetic protein receptors. *Mammalian Genome* **10,** 299-302.

Bau, Z.-Z. and Cepko, C.L. (1997) The expression and function of *Notch* pathway genes in the developing rat eye. *J. Neurosci*. **17**, 1425-1434.

Bitgood, M. J. and McMahon, A. P. (1995). Hedgehog and Bmp genes are coexpressed at many diverse sites of cell- cell interaction in the mouse embryo. *Dev. Biol.* **172,** 126-138.

Caplan, A. I. and Pechack, D.G. (1987). The cellular and molecular embryology of bone formation. In *Bone and Mineral Research*. Vol. 5 (ed. W.A Peck), pp. 117-183. New York, NY: Elsevier.

Dewulf, N., Verschueren, K., Lonnoy, O., Moren, A., Grimsby, S., Vande Spiegle, K., Miyazono, K., Huylebroeck, D. and Ten Dijke, P. (1995). Distinct spatial and temporal expression patterns of two type I receptors for bone morphogenetic proteins during mouse embryogenesis. *Endocrinology* **136,** 2652-2663.

Dunn, N. R., Winnier, G. E., Hargett, L. K., Schrick, J. J., Fogo, A. B. and Hogan, B. L. M. (1997). Haploinsufficient phenotypes in *Bmp4* heterozygous null mice and modification by mutations in *Gli3* and *Alx4*. *Dev. Biol.* **188,** 235-247.

Dymecki, S. M. (1996). Flp recombinase promotes site-specific DNA recombination in embryonic stem cells and transgenic mice. *Proc. Natl. Acad. Sci. USA* **93,** 6191-6196.

Enomoto-Iwamoto, M., Iwamoto, M., Mukudai, Y., Kawakami, Y., Nohno, T., Higuchi, Y., Takemoto, S., Ohuchi, H., Noji, S. and Kurisu, K. (1998). Bone morphogenetic protein signaling is required for maintenance of differentiation phenotype, control of proliferation, and hypertrophy of chondrocytes. *J. Cell Biol.* **140,** 409-418.

Francis-West, P. H., Abdelfattah, A., Chen, P., Allen, C., Parish, J., Ladher, R., Allen, S., MacPherson, S., Luyten, F. P. and Archer, C. W. (1999). Mechanisms of GDF-5 action during skeletal development. *Development* **126,** 1305-1315.

Freytag, S., and Geddes, T. (1992). Reciprocal regulation of adipogenesis by Myc and C/EBPalpha. *Science* **256,** 379-382.

Green, M. C. (1968). Mechanism of the pleiotropic effects of the short ear mutant gene in the house mouse. *J. Exp. Zool.* **167,** 129-150.

Gruneberg, H., and Lee, A. J. (1973). The anatomy and development of brachypodism in the mouse. *J. Embryol. Exp. Morph.* **30,** 119-141.

Hinchliffe, J. R. (1994). Evolutionary developmental biology of the tetrapod limb. *Development* **1994 Supplement,** 163-168.

Hogan, B. L. M. (1996). Bone morphogenetic proteins: multifunctional regulators of vertebrate development. *Genes Dev.* **10,** 1580-1594.

Hoodless, P. A., Haerry, T., Abdollah, S., Stapleton, M., O'Connor, M. B., Attisano, L. and Wrana, J. L. (1996). MADR1, a MAD-related protein that functions in BMP2 signaling pathways. *Cell* **85,** 489-500.

Hotten, G. C., Matsumoto, T., Kimura, M., Bechtold, R. F., Kron, R., Ohara, T., Tanaka, H., Satoh, Y., Okazaki, M., Shirai, T., Pan, H., Kawai, S., Pohl, J. S. and Kudo, A. (1996). Recombinant human growth/differentiation factor 5 stimulates mesenchymal aggregation and chondrogenesis responsible for the skeletal development of limbs. *Growth Factors* **13,** 65-74.

Hui, C. C., Slusarski, D., Platt, K. A., Holmgren, R. and Joyner, A. L. (1994). Expression of three mouse homologs of the Drosophila segment polarity gene cubitus interruptus, Gli, Gli-2, and Gli-3, in ectoderm- and mesoderm-derived tissues suggests multiple roles during postimplantation development. *Dev. Biol.* **162,** 402-413.

Hynes, M., Stone, D. M., Dowd, M., Pitts-Meek, S., Goddard, A., Gurney, A. and Rosenthal, A. (1997). Control of cell pattern in the neural tube by the zinc finger transcription factor and oncogene Gli-1. *Neuron* **19,** 15-26.

Ide, H., Saito-Ohara, F., Ohnami, S., Osada, Y., Ikeuchi, T., Yoshida, T. and Terada, M. (1998). Assignment of the BMPR1A and BMPR1B genes to human chromosome 10q22.3 and 4q23-q24 by in situ hybridization and radiation hybrid mapping. *Cytogenet. Cell Genet.* **81,** 285-286.

Kang, S., Graham, J. M., Jr., Olney, A. H. and Biesecker, L. G. (1997). GLI3 frameshift mutations cause autosomal dominant Pallister-Hall syndrome. *Nat. Genet.* **15,** 266-268.

Kawakami, Y., Ishikawa, T., Shimabara, M., Tanda, N., Enomoto-Iwamoto, M., Iwamoto, M., Kuwana, T., Ueki, A., Noji, S. and Nohno, T. (1996). BMP signaling during bone pattern determination in the developing limb. *Development* **122,** 3557-3566.

Kengaku, M., Capdevila, J., Rogriguez-Esteban, C., De La Pena, J., Johnson, R. L., Belmonte, J. C. I. and Tabin, C. J. (1998). Distinct WNT pathways regulating AER formation and dorsoventral polarity in the chick limb bud. *Science* **280,** 1274-1277.

Kingsley, D. M. (1994). What do BMPs do in mammals? Clues from the mouse short-ear mutation. *Trends Genet.* **10,** 16-21.

Lee, J., Platt, K. A., Censullo, P. and Ruiz i Altaba, A. (1997). Gli1 is a target of Sonic hedgehog that induces ventral neural tube development. *Development* **124,** 2537-2552.

Lee, K., Lanske, B., Karaplis, A. C., Deeds, J. D., Kohno, H., Nissenson, R. A., Kronenberg, H. M. and Segre, G. V. (1996). Parathyroid hormone-related peptide delays terminal differentiation of chondrocytes during endochondral bone development. *Endocrinology* **137,** 5109-5118.

Liu, F., Hata, A., Baker, J. C., Doody, J., Carcamo, J., Harland, R. M. and Massague, J. (1996). A human Mad protein acting as a BMP-regulated transcriptional activator. *Nature* **381,** 620-623.

Liu, F., Massague, J. and Ruiz i Altaba, A. (1998). C-terminally truncated GLI3 proteins associate with Smads. *Nature Genet.* **20,** 325-326.

Marigo, V., Johnson, R. L., Vortkamp, A., and Tabin, C. J. (1996). Sonic hedgehog differentially regulates expression of GLI and GLI3 during limb development. *Dev. Biol.* **180,** 273-283.

Martin, G. R. (1998). The roles of FGFs in the early development of vertebrate limbs. *Genes Dev.* **12,** 1571-1586.

Massague, J. (1996). TGFbeta signaling: receptors, transducers, and Mad proteins. *Cell* **85,** 947-950.

Merino, R., Ganan, Y., Macias, D., Economides, A. N., Sampath, K. T. and Hurle, J. M. (1998). Morphogenesis of digits in the avian limb is controlled by FGFs, TGFβs, and Noggin through BMP Signaling. *Dev. Biol.* **200,** 35-45.

Merino, R., Macias, D., Ganan, Y., Economides, A. N., Wang, X., Wu, Q., Stahl, N., Sampath, K. T., Varona, P. and Hurle, J. M. (1999). Expression and function of Gdf-5 during digit skeletogenesis in the embryonic chick leg bud. *Dev. Biol.* **206,** 33-45.

Mo, R., Freer, A. M., Zinyk, D. L., Crackower, M. A., Michaud, J., Heng, H. H., Chik, K. W., Shi, X. M., Tsui, L. C., Cheng, S. H., Joyner, A. L. and Hui, C. (1997). Specific and redundant functions of Gli2 and Gli3 zinc finger genes in skeletal patterning and development. *Development* **124,** 113-123.

Nishitoh, H., Ichijo, H., Kimura, M., Matsumoto, T., Makishima, F., Yamaguchi, A., Yamashita, H., Enomoto, S. and Miyazono, K. (1996). Identification of type I and type II serine/threonine kinase receptors for growth/differentiation factor-5. *J. Biol. Chem.* **271,** 21345-21352.

Nowakowski, R.S., Lewin, S.B. and Miller, M.W. (1989) Bromodeoxyuridine immunohistochemical determination of the lengths of the cell cycle and the DNA-synthetic phase for an anatomically defined population. *J. Neurocytol.* **18**, 311-318.

Oster, G. F., Shubin, N., Murray, J. D. and Alberch, P. (1988). Evolution and morphogenetic rules: the shape of the vertebrate limb in ontogeny and phylogeny. *Evolution* **42,** 862-884.

Parr, B. A., Shea, M. J., Vassileva, G. and McMahon, A. P. (1993). Mouse Wnt genes exhibit discrete domains of expression in the early embryonic CNS and limb buds. *Development* **119,** 247-61.

Radhakrishna, U., Wild, A., Grzeschik, K.-H. and Antonarakis, S. E. (1997). Mutation in *Gli3* in postaxial polydactyly type A. *Nature Genetics* **17,** 269-271.

Ruiz i Altaba, A. (1999). Gli proteins encode context-dependent positive and negative functions: implications for development and disease. *Development* **126,** 3205-3216.

Sasaki, H., Nishizaki, Y., Hui, C., Nakafuku, M. and Kondoh, H. (1999). Regulation of Gli2 and Gli3 activities by an amino-terminal repression

domain: implication of Gli2 and Gli3 as primary mediators of Shh signaling. *Development* **126,** 3915-3924.

Shubin, N. H. and Alberch, P. (1986). A Morphogenetic Approach to the Origin and Basic Organization of the Tetrapod Limb. *Evolutionary Biol.* **20,** 319-387.

St-Jacques, B., Hammerschmidt, M. and McMahon, A. P. (1999). Indian Hedgehog signaling regulates proliferation and differentiation of chondrocytes and is essential for bone formation. *Genes Dev.* **13,** 2072-2086.

Storm, E. E., Huynh, T. V., Copeland, N. G., Jenkins, N. A., Kingsley, D. M. and Lee, S. J. (1994). Limb alterations in brachypodism mice due to mutations in a new member of the TGF beta-superfamily [see comments]. *Nature* **368,** 639-643.

Storm, E. E. and Kingsley, D. M. (1996). Joint patterning defects caused by single and double mutations in members of the bone morphogenetic protein (BMP) family. *Development* **122,** 3969-3979.

Storm, E. E. and Kingsley, D. M. (1999). GDF5 Coordinates bone and joint formation during digit development. *Dev. Biol.* **209,** 11-27.

Takahashi, I., Nuckolls, G. H., Takahashi, K., Tanaka, O., Semba, I., Dashner, R., Shum, L. and Slavkin, H. C. (1998). Compressive force promotes sox9, type II collagen and aggrecan and inhibits IL-1beta expression resulting in chondrogenesis in mouse embryonic limb bud mesenchymal cells. *J. Cell Sci.* **111,** 2067-2076.

Tickle, C. (1995). Vertebrate limb development. *Curr. Opin. Genet. Dev.* **5,** 478-484.

van der Hoeven, F., Zakany, J. and Duboule, D. (1996). Gene transpositions in the *HoxD* complex reveal a hierarchy of regulatory controls. *Cell* **85,** 1025-1035.

Warot, X., Fromental-Ramain, C., Fraulob, V., Chambon, P. and Dolle, P. (1997). Gene dosage-dependent effects of the Hoxa-13 and Hoxd-13 mutations on morphogenesis of the terminal parts of the digestive and urogenital tracts. *Development* **124,** 4781-4791.

Yamashita, H.P., ten Dijke, P., Franzen, P., Miyazono, K. and Heldin, C.H. (1994) Formation of hetero-oligomeric complexes of type I and type II receptors for transforming growth factor-beta. *J. Biol. Chem.* **269**, 20172-20178.

Yamashita, H. P., ten Dijke, P., Heldin, C. H. and Miyazono, K. (1996). Bone morphogenetic protein receptors. *Bone* **19,** 569-574.

Yi, S. E., Daluiski, A., Pederson, Ron., Rosen, V. and Lyons, K. M. (2000). The type I BMP receptor BMPRIB is required for chondrogenesis in the mouse limb. *Development* **127,** 621-630.

Yokouchi, Y., Sakiyama, J., Kameda, T., Iba, H., Suzuki, A., Ueno, N. and Kuroiwa, A. (1996). BMP-2/-4 mediate programmed cell death in chicken limb buds. *Development* **122,** 3725-3734.

Zakany, J. and Duboule, D. (1999). Hox genes in digit development and evolution. *Cell Tissue Res.* **296,** 19-25.

Zou, H. and Niswander, L. (1996). Requirement for BMP signaling in interdigital apoptosis and scale formation. *Science* **272,** 738-741.

Zou, H., Wieser, R., Massague, J. and Niswander, L. (1997). Distinct roles of type I bone morphogenetic protein receptors in the formation and differentiation of cartilage. *Genes Dev.* **11,** 2191-3203.